中 国 激 光
CHINESE JOURNAL OF LASERS

Fabrication of nano-scale metallic photonic crystals using interference ablation

Zhaoguang Pang (庞兆广)[1,2], Xinping Zhang (张新平)[1*], Hongmei Liu (刘红梅)[1], and Tianrui Zhai (翟天瑞)[1]

[1] *Institute of Information Photonics Technology and College of Applied Sciences, Beijing University of Technology, Beijing* 100124, *China*

[2] *College of Physics Science and Information Engineering, Hebei Normal University, Shijiazhuang* 050024, *China*

* *Corresponding author: zhangxinping@bjut.edu.cn*

Abstract We demonstrate the fabrication and characterization of large area metallic photonic crystals (MPCs) in the form of gold nano-island grating structures. The spectroscopic properties of the MPCs characterized by the angle-resolved optical extinction spectrum measurements show strong couplings between the waveguide resonance modes and the particle plasmon resonance of the gold nanostructures, indicating the success of this fabrication method. The excellent optical responses of the nano-island MPCs with the advantages of large-area fabrication, low cost, and high speed make it show potential applications in optoelectronic devices and sensors.

OCIS codes 220.4241, 250.5403, 050.5298.

doi: 10.3788/CJL201239.s106003

1 Instroduction

Metallic photonic crystals (MPCs) are usually referred to the periodic arrangements of metallic nanostructures, such as nano-wires, nano-dots, and nanoholes. The particle plasmon resonance (PPR) of metallic nanostructures has attracted lots of attentions due to the unique light scattering and absorption properties[1-3], which is attributed to the collective oscillation of the conduction electrons of nanostructures excited by the electromagnetic field of incident light, is mainly dependent on the size[4], shape[5,6], and the surrounding environments[7]. MPCs have been used widely to exploit applications in novel optoelectronic devices[8-11] and sensors[12-14]. Different investigations have been demonstrated for the fabrication of MPCs, such as electron beam lithography[15,16], nano-imprinting lithography[17,18], and laser interference lithography combined etching technologies[19,20]. However, the complicated fabrication processes and the requirements of expensive equipments are the obvious disadvantages of these fabrication techniques. We demonstrate a simple and effective method for the fabrication of large-area MPCs in the form of periodic nano-island grating structures, which employs laser interference ablation[21] and subsequent high temperature annealing treatment. The microscopic and spectroscopic properties of the nano-island MPCs are systematically investigated by the scanning electron microscopy (SEM) characterization and angle-resolved extinction measurements, respectively.

2 Sample Preparation

The experimental setup is shown in Fig. 1, where a 266-nm pulsed-laser with an output energy of 20 mJ and a time duration of 6 ns is employed for the interference ablation. The laser beam is firstly split into two beams before being overlapped onto the sample, the angle between this two beams can be tuned to achieve the desired period defined by $d = \lambda/[2\sin(\theta/2)]$, where λ and θ are the laser wavelength and the angle between the two beams, respectively. Herein the angle is set about 45° to produce interference pattern with a period about 350 nm. Gold nanoparticles synthesized with chemical method are covered with organic ligands[22], which are dissolved in xylene with a concentration of 100 mg/mL to prepare the colloidal solution. Figures 2(a) - (d) illustrate the fabrication processes of the nano-island MPCs. The indium tin oxide (ITO) glass was first ultrasonically cleaned in acetone and then colloidal gold nanoparticles were spin-coated onto the ITO glass at a speed of 2000 r/min for 30 s, producing a uniform colloidal film as thick as 200 nm. Thereafter the colloidal film was exposed to the interference pattern of the single-shot UV laser pulse, the gold nanoparticles located at the bright fringes would be eliminated due to the in-

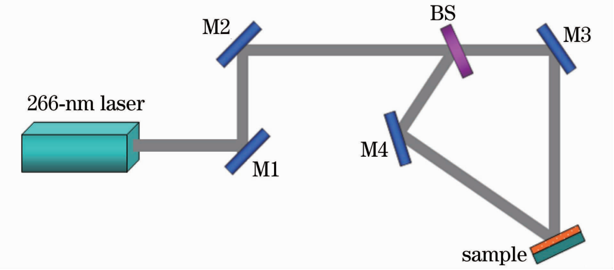

Fig. 1. Experimental setup for the interference ablation system. M1 - M4: dielectric coating mirrors

tense absorption of the organic ligands to the UV laser and gold nanoparticles located at the dark fringes would be retained, consequently the grating structures would be formed. Finally the sample were heated in a muffle furnish at the temperature of 450 ℃ for 10 min and then cool down gradually to room temperature, the high temperature annealing process enables the sublimation of the organic ligands and the formation of gold nano-islands grating structures due to the large surface energy of the melting gold.

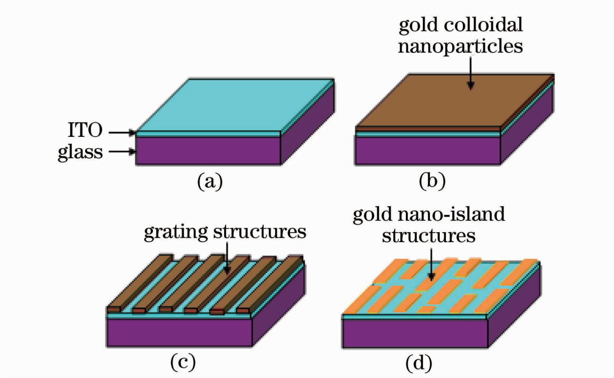

Fig. 2. Fabrication steps of the nano-island MPCs. (a) Glass substrate coated with ITO layer; (b) spin-coated gold colloidal nanoparticles onto the ITO glass; (c) grating structures formed after interference ablation; (d) gold nano-island grating structures on top of the ITO layer after high temperature annealing.

3 Microscopic characterization and spectroscopic properties

Figure 3 shows the SEM image of the grating structures after interference ablation. It can be found that uniform grating wires with a period of 350 nm have been successfully constructed. The total area of the grating wires is determined by the beam size of the UV laser, which is about 5 mm in diameter. It should be noted that under this condition the grating wires are consisted of aggregated gold nanoparticles, therefore a subsequent high temperature annealing process is employed to melt the gold nanoparticles into solid gold.

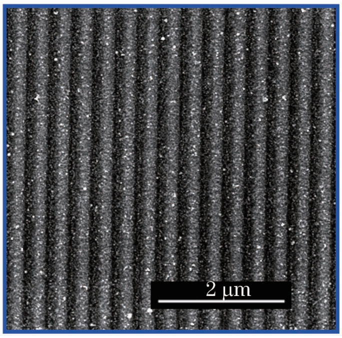

Fig. 3 SEM image of the grating structures after interference ablation.

Figure 4 shows the SEM image of the gold nano-island grating structures after annealing at 450 ℃, it can be found that the organic ligands have been sublimated completely and the nano-island MPCs structures with the same period of 350 nm have been formed.

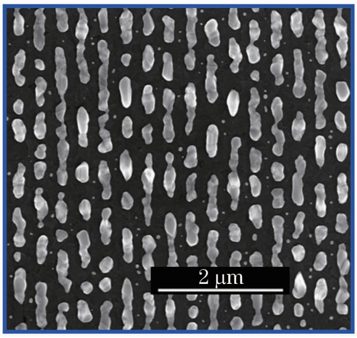

Fig. 4 SEM image of the gold nano-island MPCs.

The spectroscopic properties of the MPCs are characterized by the angle-resolved extinction spectra; the sample is mounted on a rotation stage that can rotate about the axis along the grating extending direction. A 100-W halogen lamp is used as the white-light source and a spectrometer (USB4000, Ocean Optics) is employed to measure the extinction spectra. The incident light is polarized perpendicular to the extending direction of the grating lines for the TM polarization, while the incident light is polarized parallel to the extending direction of the grating lines for the TE polarization.

Figures 5(a) and (b) show the angle-resolved optical extinction spectra for TM and TE polarizations, re-

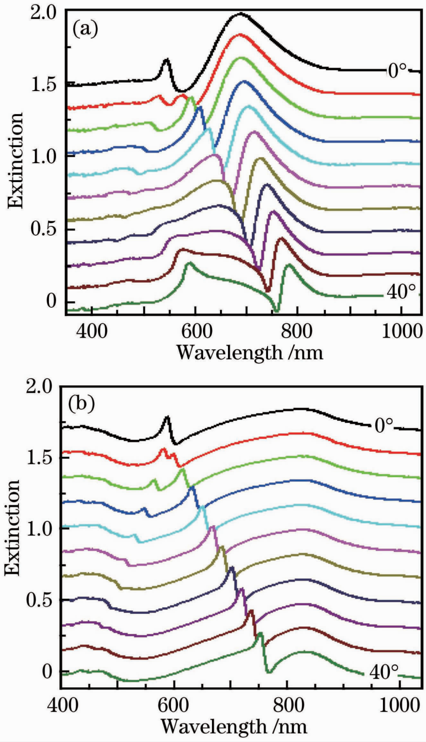

Fig. 5 Angle-resolved optical extinction measurements. (a) TM and (b) TE polarizations.

spectively. The incident angle increases from 0° to 40° with a step of 4°, strong couplings between the PPR and the waveguide resonant mode can be observed both for TM and TE polarizations. For the TM polarization, the plasmonic resonance is centered at about 685 nm with an amplitude about 0.4 optical density (OD) units and a bandwidth about 130 nm at the full width at half maximum (FWHM), the couplings between the PPR and the waveguide resonant mode can be clearly observed from Fig.5(a), which is tuned from about 570 to 755 nm when the incident angle is changed from 0° to 40°. For the TE polarization, a much broader optical extinction spectrum that centered at about 820 nm also can be observed. The amplitude of the extinction spectrum is about 0.2 OD units and a larger bandwidth about 240nm at the FWHM can be observed, the broadening of the extinction spectrum can be attributed to the irregular size distribution of the nano-islands along the direction of the grating lines. The couplings between the waveguide resonance mode and the PPR also can be found, which is tuned from about 600 to 765 nm when the incident angle is changed from 0° to 40°, as shown in Fig.5(b).

Based on the spectroscopic characterizations mentioned above, it can be found that the couplings between the PPR and the waveguide resonant mode can be excited both for the TE and TM polarizations, which are similar with the spectroscopic properties of two dimensional MPCs as reported before[23]. Therefore this unique optical response of the nano-island MPCs enhances the flexibility and extends the application scope of the one dimensional MPCs.

4 Conclusion

In conclusion, we demonstrate the fabrication of one-dimensional MPCs in the form of nano-island grating structures, where UV laser interference ablation combined subsequent high temperature annealing is employed to realize the fabrication. The optical properties of the MPCs are systematically characterized by the angle-resolved extinction measurements, strong couplings between the waveguide resonance mode and PPR are observed both for TM and TE polarizations. The unique optical response of the nano-island MPCs as well as the facile fabrication technique with the advantages of large-area, low cost, and high speed enables the potential applications in optoelectronic devices and sensors.

Acknowledgement This work was supported by the National Natural Science Foundation of China (Nos. 11074018 and 11104007), the Program for New Century Excellent Talents in University, the Research Fund for the Doctoral Program of Higher Education of China (No.20091103110012), the Beijing Educational Commission (No.KM201210005034), the Natural Science Foundation of Hebei Province (A2012205085) and the Beijing Postdoctoral Research Foundation (No.2011ZZ-22).

References

1 J. A. Fan, C. H. Wu, K. Bao, J. M. Bao, R. Bardhan, N. J. Halas, V. N. Manoharan, P. Nordlander, G. Shvets and F. Capasso, Science **328**, 1135(2010).

2 N. J. Halas, S. Lal, W. S. Chang, S. Link, and P. Nordlander, Chem. Rev. **111**, 3913(2011).

3 M. Rahmani, T. Tahmasebi, Y. Lin, B. Lukyanchuk, T. Y. F. Liew, and M. H. Hong, Nanotechnology **22**, 245204 (2010).

4 H. M. Liu, X. P. Zhang, and Z. H. Gao, Photon. Nanostruc. Fundam. Appl. **8**, 131(2010) .

5 C. Salzemann, A. Brioude, and M. P. Pileni, J. Phys. Chem. B **110**, 7208(2006).

6 U. Guler and R. Turan, Opt. Express **18**, 17322(2006)

7 K. L. Kelly, E. Coronado, L. L. Zhao, and G. C. Schatz, J. Phys. Chem. B **107**, 668(2003).

8 X. P. Zhang, B. Q. Sun, J. M. Hodgkiss, and R. H. Friend, Adv. Mater. **20**, 4455(2008).

9 X. P. Zhang, H. M. Liu, J. R. Tian, Y. R. Song, L. Wang, and G. Z. Zhang, Nanotechnol. **19**, 285202 (2008).

10 D. Nau, R. P. Bertram, K. Buse, T. Zentgraf, J. Kuhl, S. G. Tikhodeev, N. A. Gippius, and H. Giessen, Appl. Phys. B **82**, 543 (2006).

11 X. P. Zhang, H. M. Liu, J. R. Tian, Y. R. Song, and L. Wang, Nano Lett. **8**, 2653 (2008).

12 W. Kubo and S. Fujikawa, Nano Lett. **11**, 8 (2011).

13 D. Nau, A. Seidel, R. B. Orzekowsky, S. H. Lee, S. Deb, and H. Giessen, Opt. Lett. **35**, 3150 (2010).

14 X. P. Zhang, F. Dou, and H. M. Liu, Nanotechnol. **21**, 335501 (2010).

15 S. A. Kim, K. M. Byun, K. Kim, S. M. Jang, K. Ma, Y. Oh, D. Kim, S. G. Kim, M. L. Shuler, and S. J. Kim, Nanotechnol. **21**, 355503 (2010).

16 J. Henson, J. DiMaria, and R. Paiella, J. Appl. Phys. **106**, 093111 (2009).

17 C. C. Liang, M. Y. Liao, W. Y. Chen, T. C. Cheng, W. H. Chang, and C. H. Lin, Opt. Express **19**, 4768 (2011).

18 S. Buzzi, M. Galli, M. Agio, and J. F. Loffler, Appl. Phys. Lett. **94**, 223115 (2009).

19 F. Ma, M. H. Hong, and L. S. Tan, Appl Phys A **93**, 907 (2008).

20 H. C. Guo, D. Nau, A. Radke, X. P. Zhang, J. Stodolka, X. L. Yang, S. G. Tikhodeev, N. A. Gippius, and H. Giessen, Appl. Phys. B **81**, 271 (2005).

21 Z. G. Pang and X. P. Zhang, Nanotechnol. **22**, 145303 (2011).

22 X. P. Zhang, B. Q. Sun, R. H. Friend, H. C. Guo, D. Nau, and H. Giessen, Nano Lett. **6**, 651 (2006).

23 X. P. Zhang, B. Q. Sun, H. C. Guo, N. Tetreault, H. Giessen, and R. H. Friend, Appl. Phys. Lett. **90**, 133114 (2007).